



AFRL-RX-WP-TP-2009-4354

**EFFECTS OF PHASE CHANGE AND OXYGEN
PERMEABILITY IN OXIDE SCALES ON OXIDATION
KINETICS OF ZrB_2 AND HfB_2 (POSTPRINT)**

Triplicane A. Parthasarathy, Robert A. Rapp, Mark Opeka, and Ronald J. Kerans

**Ceramics Branch
Metals, Ceramics, and NDE Division**

NOVEMBER 2009

Approved for public release; distribution unlimited.

See additional restrictions described on inside pages

STINFO COPY

© 2009 The American Ceramic Society

**AIR FORCE RESEARCH LABORATORY
MATERIALS AND MANUFACTURING DIRECTORATE
WRIGHT-PATTERSON AIR FORCE BASE, OH 45433-7750
AIR FORCE MATERIEL COMMAND
UNITED STATES AIR FORCE**

NOTICE AND SIGNATURE PAGE

Using Government drawings, specifications, or other data included in this document for any purpose other than Government procurement does not in any way obligate the U.S. Government. The fact that the Government formulated or supplied the drawings, specifications, or other data does not license the holder or any other person or corporation; or convey any rights or permission to manufacture, use, or sell any patented invention that may relate to them.

This report was cleared for public release by the USAF 88th Air Base Wing (88 ABW) Public Affairs Office (PAO) on 20 May 2009 and is available to the general public, including foreign nationals. Copies may be obtained from the Defense Technical Information Center (DTIC) (<http://www.dtic.mil>).

AFRL-RX-WP-TP-2009-4354 HAS BEEN REVIEWED AND IS APPROVED FOR PUBLICATION IN ACCORDANCE WITH THE ASSIGNED DISTRIBUTION STATEMENT.

/*Signature//

KENNETH DAVIDSON, Project Engineer
Metals Branch
Metals, Ceramics, & NDE Division
Nonmetallic Materials Division

//Signature//

MICHAEL J. KINSELLA, Chief
Ceramics Branch
Metals, Ceramics, & NDE Division

//Signature//

ROBERT MARSHALL, Asst Division Chief
Metals, Ceramics, & NDE Division
Materials and Manufacturing Directorate

This report is published in the interest of scientific and technical information exchange, and its publication does not constitute the Government's approval or disapproval of its ideas or findings.

*Disseminated copies will show “//Signature//” stamped or typed above the signature blocks.

REPORT DOCUMENTATION PAGE

Form Approved
OMB No. 0704-0188

The public reporting burden for this collection of information is estimated to average 1 hour per response, including the time for reviewing instructions, searching existing data sources, gathering and maintaining the data needed, and completing and reviewing the collection of information. Send comments regarding this burden estimate or any other aspect of this collection of information, including suggestions for reducing this burden, to Department of Defense, Washington Headquarters Services, Directorate for Information Operations and Reports (0704-0188), 1215 Jefferson Davis Highway, Suite 1204, Arlington, VA 22202-4302. Respondents should be aware that notwithstanding any other provision of law, no person shall be subject to any penalty for failing to comply with a collection of information if it does not display a currently valid OMB control number. **PLEASE DO NOT RETURN YOUR FORM TO THE ABOVE ADDRESS.**

1. REPORT DATE (DD-MM-YY) November 2009			2. REPORT TYPE Journal Article Postprint		3. DATES COVERED (From - To) 01 December 2007 – 01 November 2009					
4. TITLE AND SUBTITLE EFFECTS OF PHASE CHANGE AND OXYGEN PERMEABILITY IN OXIDE SCALES ON OXIDATION KINETICS OF ZrB ₂ AND HfB ₂ (POSTPRINT)			5a. CONTRACT NUMBER In-house							
			5b. GRANT NUMBER							
			5c. PROGRAM ELEMENT NUMBER 62102F							
6. AUTHOR(S) Triplicane A. Parthasarathy (UES, Inc.) Robert A. Rapp (The Ohio State University) Mark Opeka (Naval Surface Warfare Center) Ronald J. Kerans (AFRL/RXLN)			5d. PROJECT NUMBER 5220							
			5e. TASK NUMBER 00							
			5f. WORK UNIT NUMBER 52200002							
7. PERFORMING ORGANIZATION NAME(S) AND ADDRESS(ES) UES, Inc. Dayton, OH 45432 ----- The Ohio State University Columbus, OH 43235 ----- Naval Surface Warfare Center Carderock, MD 20817			8. PERFORMING ORGANIZATION REPORT NUMBER AFRL-RX-WP-TP-2009-4354							
			9. SPONSORING/MONITORING AGENCY NAME(S) AND ADDRESS(ES) Air Force Research Laboratory Materials and Manufacturing Directorate Wright-Patterson Air Force Base, OH 45433-7750 Air Force Materiel Command United States Air Force				10. SPONSORING/MONITORING AGENCY ACRONYM(S) AFRL/RXLN			
							11. SPONSORING/MONITORING AGENCY REPORT NUMBER(S) AFRL-RX-WP-TP-2009-4354			
12. DISTRIBUTION/AVAILABILITY STATEMENT Approved for public release; distribution unlimited.										
13. SUPPLEMENTARY NOTES Journal article published in <i>J. Am. Ceram. Soc.</i> , 92 [5] (2009). PAO Case Number: 88ABW-2009-2154; Clearance Date: 20 May 2009. © 2009 The American Ceramic Society. The U.S. Government is joint author of this work and has the right to use, modify, reproduce, release, perform, display, or disclose the work. Paper contains color.										
14. ABSTRACT A wide range of experimental data on the oxidation of ZrB ₂ and HfB ₂ as a function of temperature (800 °C–2500 °C) is interpreted using a mechanistic model that relaxes two significant assumptions made in prior work. First, inclusion of the effect of volume change associated with monoclinic to tetragonal phase change of the MeO ₂ phases is found to rationalize the observations by several investigators of abrupt changes in weight gain, recession, and oxygen consumed, as the temperature is raised through the transformation temperatures for ZrO ₂ and HfO ₂ . Second, the inclusion of oxygen permeability in ZrO ₂ is found to rationalize the enhancement in oxidation behavior at very high temperatures (>1800 °C) of ZrB ₂ , while the effect of oxygen permeability in HfO ₂ is negligible. Based on these considerations, the significant advantage of HfB ₂ over ZrB ₂ is credited to the higher transformation temperature and lower oxygen permeability of HfO ₂ compared with ZrO ₂ .										
15. SUBJECT TERMS										
16. SECURITY CLASSIFICATION OF:			17. LIMITATION OF ABSTRACT: SAR		18. NUMBER OF PAGES 14		19a. NAME OF RESPONSIBLE PERSON (Monitor) Kenneth E. Davidson			
a. REPORT Unclassified							b. ABSTRACT Unclassified		c. THIS PAGE Unclassified	

Effects of Phase Change and Oxygen Permeability in Oxide Scales on Oxidation Kinetics of ZrB_2 and HfB_2

Triplicane A. Parthasarathy[†]

UES Inc., Dayton, Ohio 45432

Robert A. Rapp

The Ohio State University, Columbus, Ohio 43235

Mark Opeka

Naval Surface Warfare Center, Carderock, Maryland 20817

Ronald J. Kerans

Air Force Research Laboratory, Materials and Manufacturing Directorate, AFRL/MLLN, Wright-Patterson AFB, Ohio 45433-7817

A wide range of experimental data on the oxidation of ZrB_2 and HfB_2 as a function of temperature (800°–2500°C) is interpreted using a mechanistic model that relaxes two significant assumptions made in prior work. First, inclusion of the effect of volume change associated with monoclinic to tetragonal phase change of the MeO_2 phases is found to rationalize the observations by several investigators of abrupt changes in weight gain, recession, and oxygen consumed, as the temperature is raised through the transformation temperatures for ZrO_2 and HfO_2 . Second, the inclusion of oxygen permeability in ZrO_2 is found to rationalize the enhancement in oxidation behavior at very high temperatures (>1800°C) of ZrB_2 , while the effect of oxygen permeability in HfO_2 is negligible. Based on these considerations, the significant advantage of HfB_2 over ZrB_2 is credited to the higher transformation temperature and lower oxygen permeability of HfO_2 compared with ZrO_2 .

Nomenclature

Symbol

$\Delta W/A$ (kg/m ²)	net change in weight per unit area
W_{O_2}/A (kg/m ²)	weight of O_2 consumed per unit area
X (m)	recession of MeB_2
L (m)	thickness of zirconia region in the scale
h (m)	thickness of zirconia scale over which $\text{B}_2\text{O}_3(l)$ is present
h_{ext} (m)	external thickness of $\text{B}_2\text{O}_3(l)$
T (K)	temperature
t (s)	time
M_i (kg/mol)	molecular weight of species i
ρ_i (kg/m ³)	density of species i
f	effective fraction of pores in MeO_2 that is permeable to gas
ϕ	pore volume fraction
τ	tortuosity factor

N. S. Jacobson—contributing editor

r_p (m)	pore radius
η_i (Pa · s)	viscosity of species i
J_i (mol (m ² · s) ⁻¹)	flux of species i
Π (mol (m · s · atm) ⁻¹)	permeability coefficient of oxygen in liquid boria
α	effective evaporation coefficient
P_i (atm)	partial pressure of species i
Γ (mol (m ² · s) ⁻¹)	rate of addition of boria to the external boria scale
$J_{\text{evap},i}$ (mol (m ² · s) ⁻¹)	rate of evaporation of species i at the external surface
D_i (m ² /s)	diffusivity of species i
$D_{1,(2, \dots, i)}$ (m ² /s)	diffusivity of species 1 in a multicomponent gas mixture
$D_{\text{O}_2, \text{MeO}_2}$ (m ² /s)	diffusivity of oxygen in MeO_2
D_k (m ² /s)	Knudsen diffusivity
C_i (mol/m ³)	concentration of species i
q	h/L
F (A · s/mol)	Faraday constant
σ_{O} ($\Omega^{-1} \cdot \text{m}^{-1}$)	oxygen ionic conductivity
σ_h ($\Omega^{-1} \cdot \text{m}^{-1}$)	hole conductivity
<i>Superscripts</i>	
a	ambient
zb	zirconia–boria interface
s	MeB_2 – MeO_2 interface
i	$\text{B}_2\text{O}_3(l)$ – $\text{B}_2\text{O}_3(g)$ interface

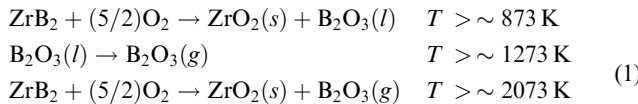
I. Introduction

DIBORIDES of Zr and Hf are now well recognized as the most promising refractory materials that are resistant to environmental degradation in air at very high temperatures, especially with SiC additions.^{1–4} However, little or no work has been reported on quantitative models of oxidation for this class of materials. A few recent works focused on thermodynamic studies,^{1,5} which have identified the key condensed and gaseous oxidation products. Modeling the kinetics of oxidation for this class of materials has been the focus of our research program. Experimental data on the kinetics of oxidation of SiC-containing diborides are only beginning to appear in the literature, while a large body of data exist on the pure diborides.^{6–11} Existence of this large data base combined with the simpler scale morphology, make modeling the oxidation of the pure diborides, the logical first step toward understanding this class of materials.

Manuscript No. 25581. Received December 2, 2008; approved February 9, 2009.
This work was supported in part by USAF Contract # FA8650-04-D-5233.

[†]Author to whom correspondence should be addressed. e-mail: triplicane.parthasarathy@wpafb.af.mil

From an initial study, we reported on a model for the oxidation of these materials in the intermediate temperature regime, *viz.* $\sim 1000\text{--}1800^\circ\text{C}$.¹² We later extended this to other temperatures.¹³ By comparing the models with the experimental data, we showed that the data can be interpreted by a model that assumes the formation of a porous zirconia, whose pores tend to be filled with liquid boria(*l*), with the boria(*l*) evaporating as $\text{B}_2\text{O}_3(\text{g})$ at higher temperatures.



Below 1273 K, the model predicted an external boria to form and it showed that inclusion of its flow was important to rationalize data at temperatures above ~ 1073 K. Above 1273 K, the boria evaporation was predicted to be significant resulting in a porous zirconia that is partially filled with liquid boria. Above ~ 2073 K, the boria evaporation was predicted to be faster than the rate of formation of boria, resulting in the scale being essentially porous zirconia. This model helped rationalize a large portion of the data reported in the literature. However, a few important effects were not captured. In particular, it is found that these works could not rationalize some of the abrupt transitions observed in the high temperature data, as reported in the literature. These transitions occur around 1400 K for ZrB_2 , and around 2000 K for HfB_2 . Second the recession rates reported by Clougherty in air at temperatures above ~ 2273 K were found to be significantly larger than was predicted by the model for ZrB_2 . Third, the model could not simultaneously predict both the weight gain and oxygen consumed reported for low temperatures (1273–1473 K) for ZrB_2 by Tripp and Graham.

In this work, we retain all elements of the prior model, but relax two of the assumptions. First, we show that by including the effect of the phase transformation of the MeO_2 oxide scale from monoclinic to tetragonal with accompanying volume change, the abrupt transitions observed in reported experimental data can be predicted/rationalized accurately. Inclusion of this mechanism is also found to be important in obtaining good predictions of both the weight gain and oxygen consumed simultaneously for ZrB_2 . Including the permeation of oxygen through the MeO_2 oxide is shown to rationalize the acceleration in oxidation at the very high temperatures for ZrB_2 , while this oxygen flux contribution is shown to be negligible for the case of HfB_2 .

The experimental data on these materials come from a variety of sources that used different methods to characterize the kinetics, *viz.*, weight gain, interface recession and/or, oxygen consumed. The materials have also been studied under a variety of different environmental conditions and temperature regimes. The model is able to rationalize all of these data.

II. The Model

The key elements of the model described in detail in our earlier work are retained.¹² As a brief overview, a schematic of the general model is shown in Fig. 1, which illustrates the assumed morphology of the oxidation products, representing steady-state conditions. The assumptions are based on experimental observations as noted in our prior work.¹² The oxidation product, *viz.*, the scale, consists of MeO_2 and liquid boria, with $\text{B}_2\text{O}_3(\text{g})$ as the dominant gaseous species. At low temperatures where the vapor pressure of B_2O_3 is very low, the pores between the columnar MeO_2 product are filled with liquid boria, which is retained by the low-surface tension and good wettability of MeO_2 by boria. At low temperatures the scale supports an external boria film. This external boria that forms at low temperatures can flow under gravity or due to shear forces from external fluid flow. Oxygen diffuses through the external boria layer and then through the tortuous pathway between zirconia grains to reach the substrate.

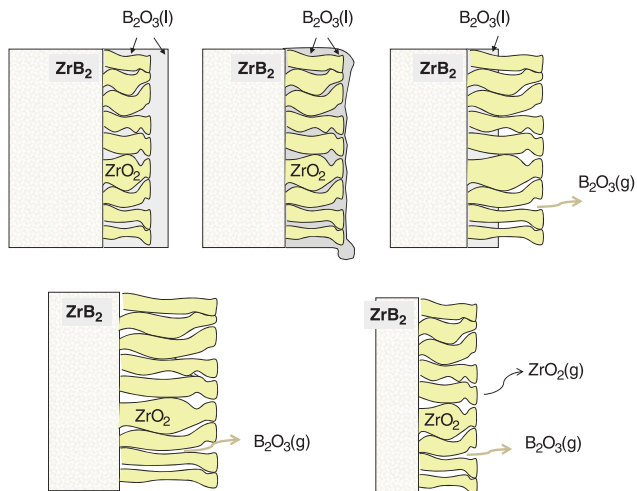


Fig. 1. Schematic sketch of the oxidation products and morphology assumed in the model. The progression of the cartoons represents steady state for increasing temperature.

As the temperature is raised, volatilization as $\text{B}_2\text{O}_3(\text{g})$ results in loss of the external boria film, so that the porous channels of the MeO_2 scale are then partially filled with liquid boria. Gaseous oxygen must then diffuse through the outer part of the zirconia pore channel, and then permeate through the boria in the base of pore channel to reach the substrate. The model assumes that a quasi-steady state is reached where the rate of boria formation is balanced by the rate of boria evaporation, which determines the depth to which the zirconia pores are filled with boria. At yet higher temperatures, where boria evaporates as fast as it forms so that liquid boria is absent in the pores, oxidation is limited by gaseous diffusion of oxygen in the pores, which has a weak temperature dependence. In addition, the evaporation of MeO_2 becomes significant resulting in a reduction in the oxide scale thickness. This enhances the oxidation rate, and is therefore taken into account.

Thus the rate-limiting step for oxidation at intermediate temperature is the permeation of oxygen through liquid boria in series with gaseous diffusion of oxygen through porous open channels. Oxygen permeation through solid MeO_2 is negligible at low and intermediate temperatures, due to the low electronic conductivity of ZrO_2 and HfO_2 . Diffusion in the pores is assumed to follow Fick's law, and kinetic laws are derived for planar symmetry.

In this work, we retain derivations from our prior model for the low-temperature regime, but relax two of the assumptions, one in the intermediate temperature regime ($\sim 1273\text{--}2073$ K) and another in the high-temperature regime (above ~ 2073 K). In the intermediate temperature regime, we rationalize the effect of the phase change of MeO_2 from monoclinic to tetragonal to effect a change in the effective porosity of the scale (Fig. 2). The transformation results in volumetric shrinkage with increasing temperature. We suggest that the monoclinic MeO_2 nucleates and grows during the transient heat up of the sample; as the sample crosses the transformation temperature the MeO_2 in the scale transforms to tetragonal, shrinking in the process and expanding the gap between the MeO_2 grains. Thus we introduce an increase in porosity of the scale at the transformation temperature, and we assume that this higher porosity is retained during further oxidation. Second, at very high temperatures when the scale is free of boria (typically above ~ 2073 K), the permeation of oxygen ions through the MeO_2 is considered and included in the total flux of oxygen through the oxidation scale.

(1) Model Equations

The present work extends that detailed in Parthasarathy *et al.*^{12,13} The reader is referred to those works for detailed derivations. Here the derivations are limited to what is new; but for 2

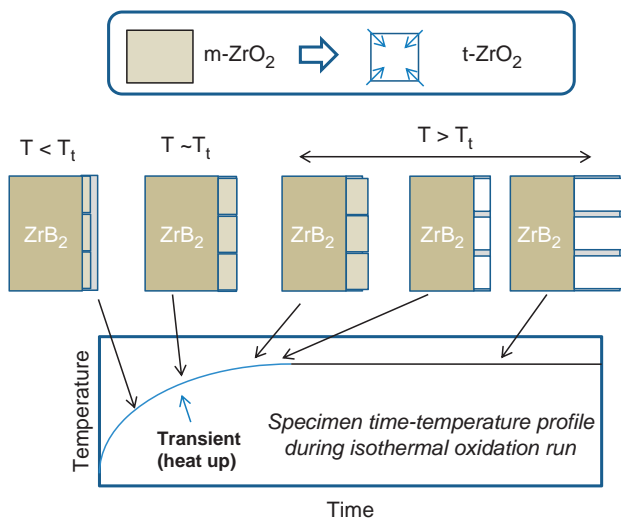


Fig. 2. A schematic sketch showing the model assumptions. During transient heat-up the oxide scale consists of *m*-ZrO₂. As the temperature rises above the transformation temperature, the *m*-ZrO₂ converts to *t*-ZrO₂ with an associated shrinkage, which opens up the pathway for oxygen permeation, enhancing oxidation. The model assumes that this opening remains constant as oxidation continues to thicken the scale.

continuity, equations derived in our prior work^{12,13} and used in this work are briefly summarized. All the model variables are listed and defined in the nomenclature.

The following shows equations for the three different regimes. In all regimes, the diffusivity of gases in a multicomponent gas mixture and the effect of Knudsen diffusion were modeled as detailed in Parthasarathy *et al.*¹² At the outer surface, either boria or MeO₂ evaporation takes place under boundary-layer-limited diffusion. This evaporation at the surface of species *i*, with molecular weight *M_i*, at partial pressure *P_i*, at temperature *T*, was taken to follow the modified Langmuir law that includes the effect of boundary layer as follows:

$$J_{\text{evap},i} = \alpha P_i / (2\pi M_i RT)^{0.5} \quad (2)$$

where α represents the effect of boundary-layer-limited diffusion, and varies with experimental conditions, but is reported to be in the range of 10^{-3} – 10^{-2} under most laboratory conditions.¹⁴ A value of 5×10^{-3} was used for all model results shown in this work.

(*A*) *High-Temperature Regime:* As pointed out in Parthasarathy *et al.*,¹² the permeabilities of oxygen through zirconia and hafnia at high-oxygen activities are dominated by electron-hole conductivity, which is much lower than the ionic conductivity except at very high temperatures. Thus assuming that MeO₂ is inert to oxygen permeation in the intermediate temperature regime, as carried out in Parthasarathy *et al.*,¹² was a good assumption. However, at very high temperatures, above ~ 2000 K, the hole conductivity becomes significant and oxygen permeation through MeO₂ must be taken into account. In this work, the model for the high-temperature regime presented in Parthasarathy *et al.*¹³ is modified to include this effect.

The effect of diffusion of oxygen through the zirconia phase in the scale was taken into account as follows. As elaborated in Parthasarathy *et al.*,¹² for ZrO₂, the ionic and hole conductivities were taken as

$$\sigma_0(\Omega^{-1} m^{-1}) = \frac{[C_{\text{dopant}}]}{0.15} 2.323 \times 10^5 \exp\left(-\frac{123\,500}{8.314}\right) \quad (3)$$

$$\sigma_h(P_{\text{O}_2})(\Omega^{-1} m^{-1}) = (P_{\text{O}_2})^{1/4} \left(\frac{[C_{\text{dopant}}]}{0.15}\right)^{1/2} 2.328 \times 10^6 \exp\left(-\frac{235\,200}{8.314}\right) \quad (4)$$

where C_{dopant} is the trivalent dopant (impurity) concentration in the MeO₂, σ_0 is the ionic conductivity, and $\sigma_h(P_{\text{O}_2})$ is the hole conductivity of ZrO₂ at partial pressure of oxygen, P_{O_2} . The oxygen diffusivity in hafnia has been reported to be a factor of about 5 lower than that of zirconia.¹⁵ Thus the ionic conductivity of hafnia was taken to be one-fifth that of zirconia.

Noting that the ionic conductivity is known to be P_{O_2} independent and hole conductivity has a $(P_{\text{O}_2})^{1/4}$ dependence, the flux of oxygen through the oxide, MeO₂, is now given by Wagner's equation as,¹⁶

$$|J_{\text{O}_2, \text{MeO}_2}| = \frac{1-f}{L} \frac{RT}{16F^2} \int_{P_{\text{O}_2}^a}^{P_{\text{O}_2}^s} \frac{\sigma_{\text{ion}} \sigma_h}{\sigma_{\text{ion}} + \sigma_h} d \ln P_{\text{O}_2} \quad (5)$$

where $P_{\text{O}_2}^a$ and $P_{\text{O}_2}^s$ are the oxygen partial pressures at the ambient and at the oxide/boride interface, and f is the fraction of pores in the oxide. Combining Eqs. (3), (4), and (5) and integrating, one obtains

$$|J_{\text{O}_2, \text{MeO}_2}| = \frac{1-f}{L} \frac{RT}{4F^2} \sigma_0 \ln \frac{\sigma_h(P_{\text{O}_2}^a) + \sigma_0}{\sigma_h(P_{\text{O}_2}^s) + \sigma_0} \quad (6)$$

where σ_0 , $\sigma_h(P_{\text{O}_2}^a)$ are given by Eqs. (3) and (4). The parallel flux of oxygen through the gas phase in the pores is given as

$$|J_{\text{O}_2, \text{gas}}| = f D_{\text{O}_2} \frac{C_{\text{O}_2}^a - C_{\text{O}_2}^s}{L} \quad (7)$$

The net flux of oxygen to the MeB₂/MeO₂ interface, and its relation to flux of B₂O₃ and formation rate of MeO₂, is given by

$$(|J_{\text{O}_2, \text{MeO}_2}| + |J_{\text{O}_2, \text{gas}}|) \frac{2}{5} = |J_{\text{B}_2\text{O}_3}| = \dot{n}_{\text{MeO}_2} \quad (8)$$

where

$$|J_{\text{B}_2\text{O}_3}| = f D_{\text{B}_2\text{O}_3} \frac{P_{\text{B}_2\text{O}_3}^s - P_{\text{B}_2\text{O}_3}^a}{RTL} 10^5 \quad (9)$$

$$P_{\text{B}_2\text{O}_3}^s = K_{\text{reaction}} P_{\text{O}_2}^{s/2} \quad (10)$$

where D_{O_2} , $D_{\text{B}_2\text{O}_3}$ are the gas phase diffusivities of oxygen and B₂O₃ through the pores, and K_{reaction} is the chemical equilibrium constant for the reaction, $\text{MeB}_2 + 5/2\text{O}_2 \rightarrow \text{MeO}_2 + \text{B}_2\text{O}_3(g)$.

Equation (7) along with Eqs. (5), (6) and (8), (9) can be solved numerically for $P_{\text{B}_2\text{O}_3}^s$ and $P_{\text{O}_2}^s$. These values were then used in the following differential equation, which was numerically integrated to obtain scale thickness L , recession X , weight-gain per unit area $\Delta W/A$, and weight of oxygen consumed per unit area W_{O_2}/A .

$$\frac{dL}{dt} = \left(\frac{1}{1-f}\right) \left[\frac{2}{5} (|J_{\text{O}_2, \text{MeO}_2}| + |J_{\text{O}_2}|) - J_{\text{evap}, \text{ZrO}_2} \right] \times \frac{M_{\text{MeO}_2}}{\rho_{\text{MeO}_2}} \quad (11)$$

$$\frac{dX}{dt} = \frac{2}{5} (|J_{\text{O}_2, \text{MeO}_2}| + |J_{\text{O}_2}|) \frac{M_{\text{MeB}_2}}{\rho_{\text{MeB}_2}} \quad (12)$$

$$\frac{\Delta W}{A} = L\rho_{\text{MeO}_2}(1-f) - X\rho_{\text{MeB}_2} \quad (13)$$

$$\frac{W_{\text{O}_2}}{A} = \frac{5}{2} \times \frac{M_{\text{O}_2}}{M_{\text{MeB}_2}/\rho_{\text{MeB}_2}} \quad (14)$$

Note that the model calculates the contribution of ambipolar oxygen diffusion in the MeO_2 phases assuming that the oxide pegs retain a dense morphology of constant cross section. Thus the calculated oxygen flux contribution should be considered the maximum possible flux contribution.

(B) *Intermediate Temperature Regime*: The phase transformation of zirconia is assumed to result in a change in the effective volume fraction of pores in the zirconia. Because the transformation from monoclinic to tetragonal results in volumetric shrinkage, the fraction of pores will increase as the temperature reaches the transformation temperature. Thus in the model we have

$$\begin{aligned} f &= f_1 \text{ for } T < T_{\text{trans}} \\ f &= f_2 \text{ for } T > T_{\text{trans}} \end{aligned} \quad (15)$$

with $f_2 < f_1$. The other parameters are given by equations derived in Parthasarathy *et al.*,¹² summarized below, for the key parameters of interest, the internal depth of liquid boria, h , the zirconia scale thickness, L , recession of MeB_2 , and weight-gain per unit area, $\Delta W/A$, and weight of oxygen consumed per unit area, W_{O_2}/A

$$h = qL; \quad (16)$$

$$q = \frac{\Pi_{\text{O}_2-\text{B}_2\text{O}_3}(P_{\text{O}_2}^i - P_{\text{O}_2}^s)}{D_{\text{O}_2}(C_{\text{O}_2}^a - C_{\text{O}_2}^i) + \Pi_{\text{O}_2-\text{B}_2\text{O}_3}(P_{\text{O}_2}^i - P_{\text{O}_2}^s)} \quad (16)$$

$$L^2 = 2 \left[\frac{2}{5} \left(\frac{M_{\text{ZrO}_2}}{\rho_{\text{ZrO}_2}} \right) \left(\frac{f}{1-f} \right) D_{\text{O}_2} \frac{C_{\text{O}_2}^a - C_{\text{O}_2}^i}{(1-q)} \right] t \quad (17)$$

$$X = L(1-f) \frac{M_{\text{MeB}_2}/\rho_{\text{MeB}_2}}{M_{\text{MeO}_2}/\rho_{\text{MeO}_2}} \quad (18)$$

$$\frac{\Delta W}{A} = L\rho_{\text{MeO}_2}(1-f) + hf\rho_{\text{B}_2\text{O}_3} - X\rho_{\text{MeB}_2} \quad (19)$$

$$\frac{W_{\text{O}_2}}{A} = \frac{5}{2} \times \frac{M_{\text{O}_2}}{M_{\text{MeB}_2}/\rho_{\text{MeB}_2}} \quad (20)$$

(C) *Low-Temperature Regime*: The parameters of interest are external boria thickness, the thickness of the zirconia scale, recession, and weight gain. In the absence of viscous flow of the external boria, the effective external layer thickness is determined by the rate of production of boria less the rate of evaporation of boria. The boria included in the underlying porous zirconia layer also contributes to the effective diffusion barrier thickness.

$$\begin{aligned} h_{\text{ext}}(\text{maximum}) &= \left(L \frac{(1-f)}{(M_{\text{MeO}_2}/\rho_{\text{MeO}_2})} - J_{\text{evap(B}_2\text{O}_3)} t \right) \\ &\times \frac{M_{\text{B}_2\text{O}_3}}{\rho_{\text{B}_2\text{O}_3}} - fL \end{aligned} \quad (21)$$

When viscous flow is significant, the external boria layer thickness is decreased to a value determined by the rates at which it flows and thins at the surface, as given below. Assuming laminar flow of the boria, the “effective” external thickness, h_{ext} , is given by Perry and Chilton¹⁷

$$h_{\text{ext}} = \left[\frac{3(M_{\text{B}_2\text{O}_3}\Gamma_{\text{B}_2\text{O}_3}l_{\text{spec}})\eta_{\text{B}_2\text{O}_3}}{gp_{\text{B}_2\text{O}_3}^2 \sin(\phi)} \right]^{1/3} \quad (22)$$

where $\Gamma_{\text{B}_2\text{O}_3}$ is the number of moles of boria formed and added per unit area, per unit time, on the surface.

$$\begin{aligned} \Gamma_{\text{B}_2\text{O}_3} &= \frac{dn_{\text{ext,B}_2\text{O}_3}}{dt} \\ &= \left[\frac{dL}{dt} \frac{(1-f)}{(M_{\text{MeO}_2}/\rho_{\text{MeO}_2})} - f \frac{dL}{dt} \frac{\rho_{\text{B}_2\text{O}_3}}{M_{\text{B}_2\text{O}_3}} - J_{\text{evap,B}_2\text{O}_3} \right] \dots \end{aligned} \quad (23)$$

The MeO_2 scale thickness, recession of MeB_2 , weight-gain of the sample, and the weight of oxygen consumed are then given by

$$\frac{dL}{dt} = \frac{1}{1-f} \frac{2}{5} f \frac{\Pi_{\text{O}_2-\text{B}_2\text{O}_3}}{L} (P_{\text{O}_2}^{\text{ZB}} - P_{\text{O}_2}^s) \frac{M_{\text{MeO}_2}}{\rho_{\text{MeO}_2}} \dots \quad (24)$$

$$\begin{aligned} \frac{\Delta W}{A} &= L\rho_{\text{MeO}_2}(1-f) + (h_{\text{ext}} + fL)\rho_{\text{B}_2\text{O}_3} - X\rho_{\text{MeB}_2} \\ &\dots \end{aligned} \quad (25)$$

$$X = L(1-f) \frac{M_{\text{MeB}_2}/\rho_{\text{MeB}_2}}{M_{\text{MeO}_2}/\rho_{\text{MeO}_2}} \dots \quad (26)$$

$$\frac{W_{\text{O}_2}}{A} = \frac{5}{2} \times \frac{M_{\text{O}_2}}{M_{\text{MeB}_2}/\rho_{\text{MeB}_2}} \dots \quad (27)$$

III. Model Predictions and Validation

(1) Parameters

A list of variables used in the model as shown in the nomenclature with a brief description. The model uses data from the literature for all thermodynamic quantities, which are available in the compendium by Barin.¹⁸ The diffusivities of gases in multigas mixtures were calculated using parameters given by Svehla,¹⁹ and the methods outlined in Parthasarathy *et al.*¹² The Knudsen effect on diffusivity was included as determined by the pore radius. The temperature-dependent viscosity of boria was obtained from the works of Eppler²⁰ and Li *et al.*²¹ The permeability of oxygen in liquid boria was obtained from the works of Tokuda *et al.*²² and Luthra.²³

The only unknown parameters in the model are the pore radius, effective (tortuosity-included) volume fraction of pores before and after the phase transition of MeO_2 , and the concentration of dopants (unintentional impurities) in the MeO_2 . The pore radius was taken to be $0.5 \mu\text{m}$, which is based on microstructures reported in the literature; further parametric studies in Parthasarathy *et al.*¹² showed that there is no significant effect unless the pores are $<0.1 \mu\text{m}$ in size. The trivalent dopant concentration, C_{dopant} , in MeO_2 was taken to be 0.1% , which is reasonable given the purity levels of the diborides used in the experimental work. For the case of ZrO_2 , at the highest temperatures of the test, raising the dopant levels to 0.5% gave better fit to experimental data, implying impurities gained from the furnace atmosphere as a possible way to rationalize the data. The choice of dopant concentration had no effect on predictions for HfB_2 oxidation, implying that the effect of oxygen through the HfO_2 is negligible.

The effective volume fraction, f , of pores is determined by the actual volume fraction of pores, ϕ , and the tortuosity of the pores, τ . The tortuosity is defined as^{24,25}

$$\tau = \phi \frac{D}{D_{\text{eff}}}; \quad D = \left(\frac{1}{D_g} + \frac{1}{D_k} \right)^{-1}; \quad f = \frac{\phi}{\tau} \dots \quad (28)$$

Simulations show that the tortuosity factor is about 25 for $\phi = 0.05$, and ~ 4 for $\phi = 0.15$.²⁶ Thus the effective volume

fraction, f , can be much smaller than the actual porosity at low volume fractions of porosity. If the tortuosity is taken into account, values for the effective volume fraction, f , of 0.03–0.04 (representing $\phi \sim 0.15$), are very reasonable, compared with experimental images of the porous scale.

The effect of phase transformation of MeO_2 was estimated from published data on volume change associated with monoclinic to tetragonal phase transformations. The temperature of transformation was taken to be 1400 K for ZrO_2 and 2000 K for HfO_2 , in close agreement with the findings of the review published by Wang *et al.*,²⁷ who quote an average value of 1367 and 2052 K, respectively. The volume change associated with the transformation has been reported to be $\sim 3\%$, with the value for ZrO_2 being slightly larger than that for HfO_2 , in the review by Taylor.²⁸ The effective pore fraction, f that gave the best fit was 0.04 for ZrO_2 and 0.03 for HfO_2 , above the transformation temperature. Below the transformation temperature, the values assumed were 0.0015 and 0.003 for ZrO_2 and HfO_2 , respectively. The smaller pore fraction is attributed to the lack of phase transformation for the monoclinic phase, and the finite value of pore fraction is attributed to the low surface tension of boria (at 600°C, it is 0.07 N/m,²⁹ same as water at 25°C) that is likely to result in complete wetting of the zirconia/hafnia by liquid boria.

(2) Comparison of Model Predictions with Experimental Data

There are extensive data in the literature on the low-temperature, intermediate temperature, and high-temperature regimes of oxidation of ZrB_2 and HfB_2 , although there are a limited number

of investigators. Berkowitz-Mattuck¹⁰ has conducted extensive tests and reported on the temperature dependence of parabolic rate constants for recession and oxygen consumed using gas conductivity measurements under 37.5 torr (0.0049 MPa) partial pressure of oxygen in helium carrier gas. Weight gain and oxygen consumed as a function of time in the low-temperature regime, under 250 torr (0.033 MPa) of pure oxygen, have been reported by Tripp and Graham.¹¹ Interface recession and oxygen consumed at higher oxygen partial pressures (air) in the intermediate and high-temperature regimes have been reported by Kaufman *et al.*³⁰ For the high-temperature oxidation, the recession rates in 1 h in air were measured by Kaufman and Clougherty.^{6–8} Kaufman³⁰ has also reported on the time dependence of oxygen consumed at high temperatures in 0.005 MPa O_2 partial pressure for ZrB_2 . We examine the validity of the model by comparing with these data sets.

Figure 3 shows the data for ZrB_2 and HfB_2 , along with model predictions for recession rate constant and the parabolic rate constant for oxygen consumed. The jumps in the data are well represented by the model, thus attributing these transitions to the volumetric shrinkage upon phase change for ZrO_2 and HfO_2 . At higher temperatures, where there is no liquid boria in the scale, the model includes the diffusion of oxygen ions through the oxide in addition to gaseous diffusion through the pores. As seen from Eqs. (2) and (3) the permeation flux is dependent on the concentration of the dopant (here impurities) in the oxide. For ZrB_2 , the fit with the experimental data at the highest temperatures is good with 0.5% impurity in the oxide, indicating that the experimental samples had some impurity (not surprising) or that the samples picked up impurity from the en-

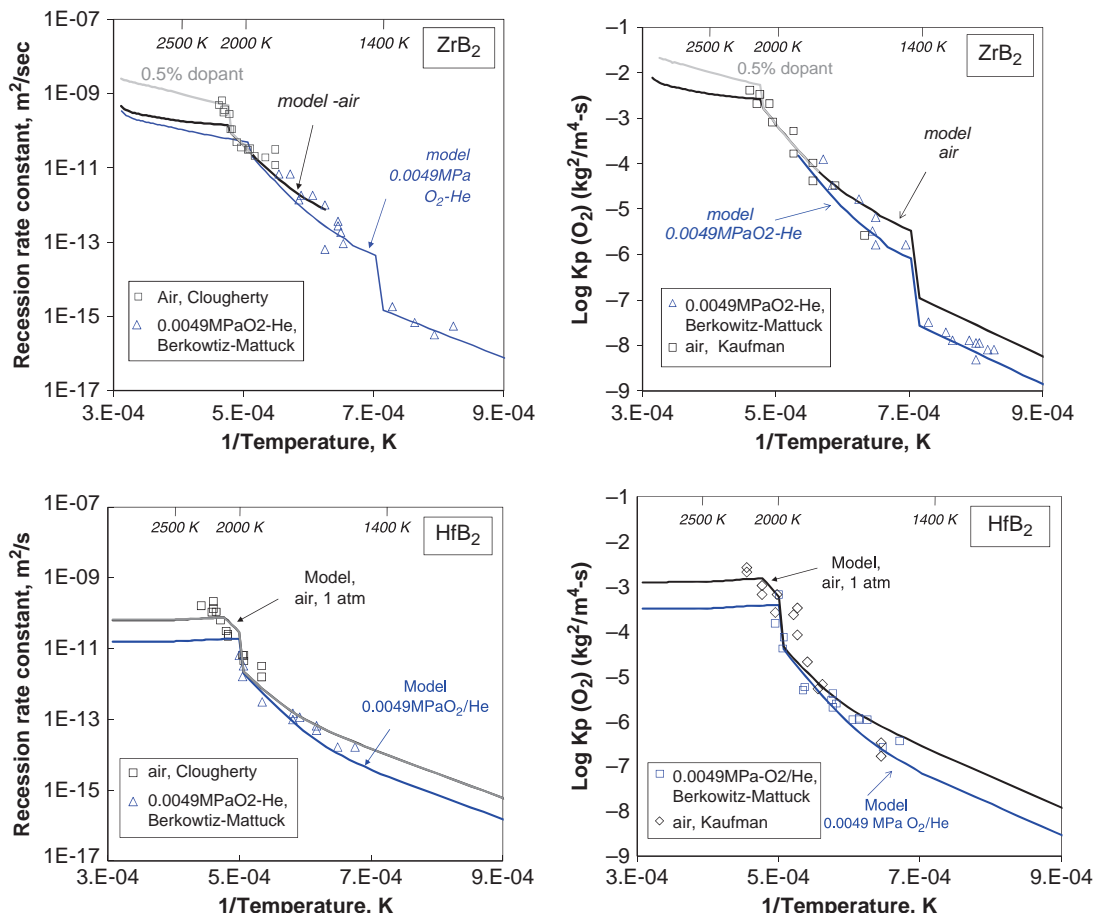


Fig. 3. The effect of phase transition of the MeO_2 , and the effect of oxygen permeation through MeO_2 at very high temperatures are shown by comparing model predictions to experimental data. The plots compare the model predictions of parabolic constants for recession and oxygen consumed as a function of temperature for ZrB_2 and HfB_2 , with experimental data reported in the literature. The model predicts the transitions based on the phase transition of ZrO_2 at 1400 K and that of HfO_2 at 2000 K, which is very close to phase transition temperatures reported in the literature. At the highest temperatures, using 0.5% dopant in ZrO_2 resulted in a better fit, while permeation of oxygen through HfO_2 was found to be negligible even at 1% dopant concentration.

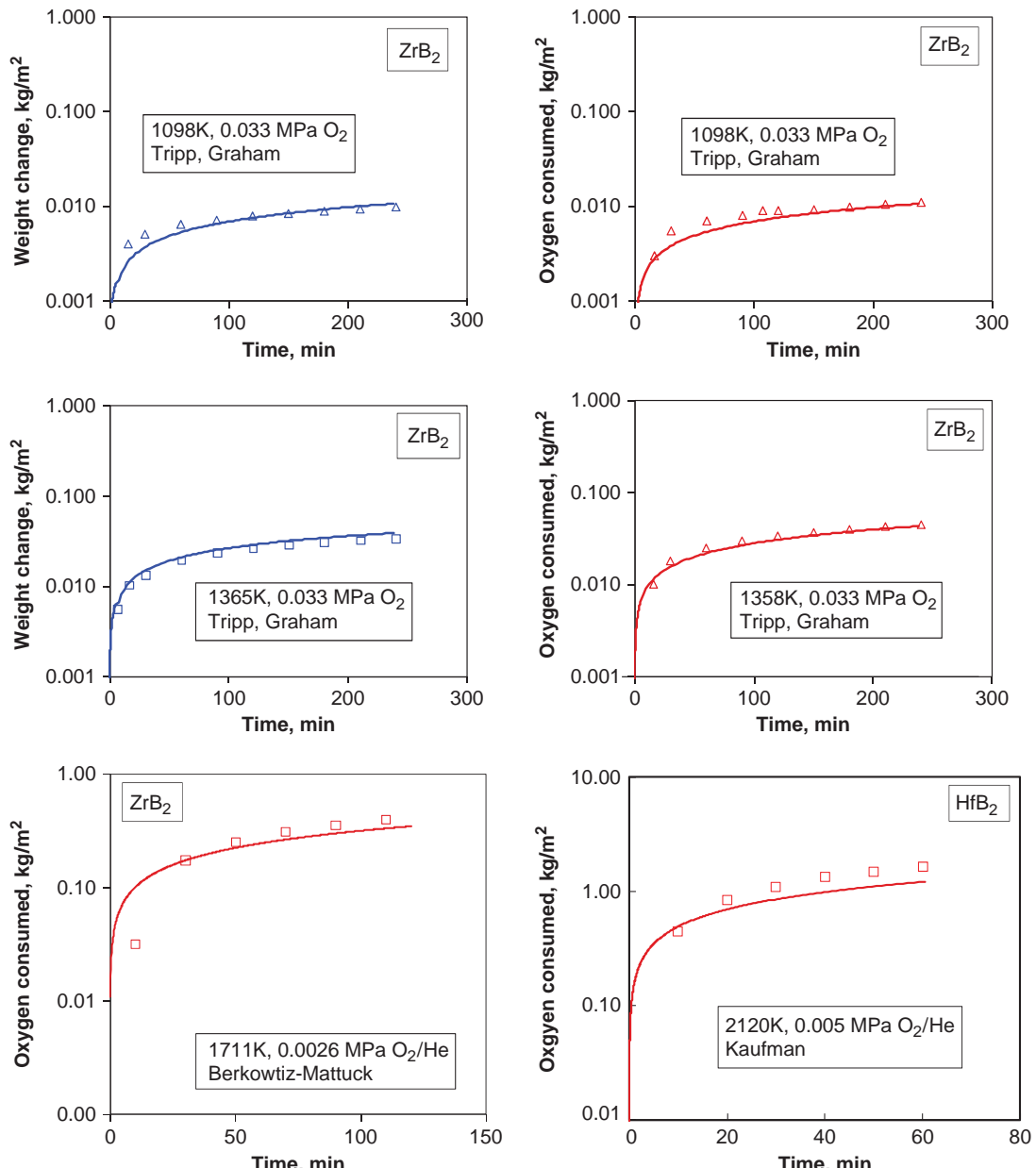


Fig. 4. Model predictions for time-dependent behavior are compared with reported data. For the low-temperature regime, the weight gain and oxygen consumed as a function of time, reported on ZrB_2 in 0.033 MPa oxygen, by Tripp and Graham are shown. For the intermediate regime, the oxygen consumed for a sample tested in 0.0026 MPa oxygen helium mixture at 1711 K is compared with the data of Berkowitz-Mattuck. For the high-temperature regime, the data for HfB_2 in 0.005 MPa O_2/He mixture of Kaufman is compared with the model prediction.

vironment during high-temperature oxidation treatments. The value chosen for impurity level had no effect on the predictions for HfB_2 , and the fit with the experimental data is good, implying that HfB_2 is insensitive to impurities.

Figure 4 shows the model predictions for time-dependent oxidation behavior in the low-temperature regime, compared with those measured by Tripp and Graham¹¹ on ZrB_2 samples under 0.033 MPa oxygen partial pressure of pure oxygen. Both the weight gain and the oxygen consumed are shown to be in good agreement indicating that the model interpretations are reasonable. The data for intermediate temperature are due to Berkowitz-Mattuck,¹⁰ and the high-temperature data on HfB_2 is from Kaufman *et al.*³⁰ The model is shown to be very reasonable under all temperature regimes.

Figure 5 shows the dependence on oxygen partial pressure predicted by the model compared with the data of Berkowitz-Mattuck for HfB_2 . The oxygen partial pressure dependence shows a transition from nearly independent at low oxygen partial pressures to nearly linear at higher partial pressures of ox-

ygen. The mechanism for this transition arises from the transition in oxygen transport being dominated by permeation through liquid boria at lower partial pressures, to diffusion of gaseous oxygen through pores in the zirconia at higher partial pressures. Thus the transition in the dependence with respect to P_{O_2} or temperature, is related to the fraction of the oxygen diffusion path along liquid boria versus gaseous pore. Higher oxygen partial pressure and lower temperatures favor retention of liquid boria and thus a linear dependence on oxygen partial pressure, as was shown in Parthasarathy *et al.*¹²

IV. Discussion

This work examined the effects of the shrinkage of the oxide scale due to phase transformation and of the higher temperature ambipolar diffusivity of oxygen in the oxide scale on the kinetics of oxidation of ZrB_2 and HfB_2 .

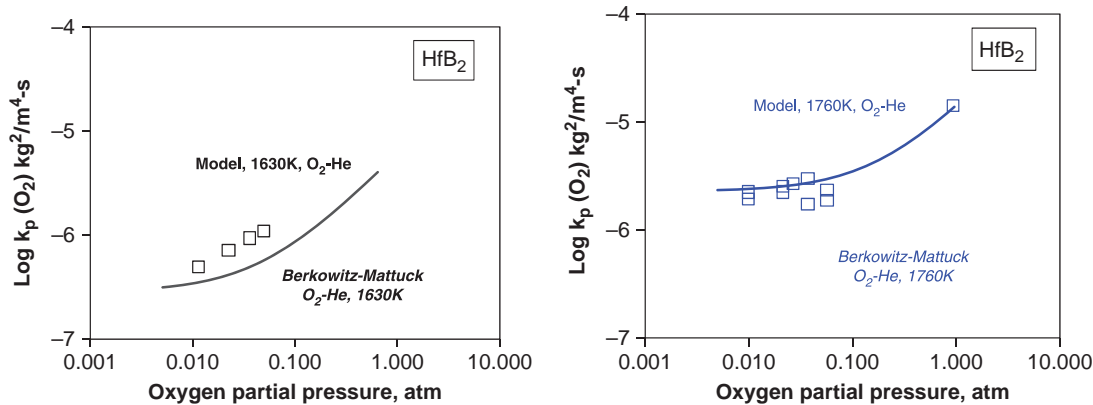


Fig. 5. The effect of oxygen partial pressure on the measured parabolic rate constant of oxygen consumed is compared with the model predictions for HfB_2 , at two different temperatures.

The model introduced the effect of phase transformation using a simple adjustment to the pore fraction in the oxide scale formed, but in proportion and magnitude to experimentally observed volume change and the actual temperature of the transformation. The agreement with experimental data are found to be very good. This suggests that the effect of phase transformation of the MeO_2 from monoclinic to tetragonal plays an important role in the oxidation kinetics of MeB_2 . The much better resistance to oxidation for HfB_2 in the temperature of experimental measurements (typically $< 1600^\circ\text{C}$, the transformation temperature of HfO_2) can be attributed entirely to the higher transformation temperature of 2000 K for HfO_2 versus 1400 K for ZrO_2 . If this is true, then additives that increase the transformation temperature or suppress the transformation temperature must be beneficial to the oxidation resistance of ZrB_2 and HfB_2 .

The model introduces the effect of ambipolar diffusion of oxygen in MeO_2 at higher temperatures using the semiempirical expressions derived in Parthasarathy *et al.*¹² This requires that a small percentage of extraneous dopant/impurity of a different valency be present in the oxide and that its amount in the scale be known. Assuming a value of 0.1% of trivalent dopants in the oxide scale is able to rationalize the high-temperature data well. For ZrB_2 , a value of 0.5% rationalizes data at the highest temperatures tested, implying the possibility of impurities picked up during oxidation. At 2273 K, the relative contribution of ambipolar diffusion of oxygen to the total oxygen permeation is about 30% at 0.1% impurity level and rises to about 60% at 0.5% impurity level. It is noteworthy that HfB_2 is insensitive to impurity level in its oxide; the relative contribution of ambipolar diffusion to total oxygen ingress is <1% at 2273 K. Once again, the better oxidation resistance of HfB_2 over ZrB_2 suggested by the model is credited to the lower diffusivity of oxygen in hafnia compared with zirconia, as reported by Smith *et al.*¹⁵ In addition, the lower vapor pressures of hafnia, minimizes evaporative loss in the extreme high-temperature regime.

In summary, a model that includes phase transformation of the oxide scale and the ambipolar diffusion of oxygen through the oxide at high temperatures is found to rationalize the experimental data reasonably well. Alloying additions that suppress or delay the phase transformation would be beneficial.

V. Summary

A wide range of experimental data on the oxidation of ZrB_2 and HfB_2 as a function of temperature from 800° to 2500°C are interpreted using a mechanistic model that relaxes two assumptions made in prior work. First, inclusion of the effect of volume change associated with monoclinic to tetragonal phase change of the MeO_2 is found to rationalize the observations by several investigators of abrupt changes in weight gain, recession and

oxygen consumed, as temperature is raised through the transformation temperature in both ZrB_2 and HfB_2 . Second, the inclusion of oxygen permeability in ZrO_2 , neglected in prior treatments, is found to help rationalize the behavior at very high temperatures ($> 1800^\circ\text{C}$) of ZrB_2 , where an enhancement in oxidation has been observed. At 2273 K, the relative contribution of ambipolar diffusion in ZrO_2 to oxygen ingress is about 30% at 1% impurity level in the oxide. The effect of oxygen permeability in HfO_2 is negligible (<1%) and thus the oxidation of HfB_2 is insensitive to trivalent impurities. Based on this analysis, the significant advantage of HfB_2 over ZrB_2 is credited to the higher transformation temperature and lower oxygen permeability of HfO_2 compared with ZrO_2 .

Acknowledgment

We acknowledge useful discussions with Dr. I. Talmy of NSWC, MD.

References

- M. M. Opeka, I. G. Talmy, and J. A. Zaykoski, "Oxidation-Based Materials Selection for 2000°C+ Hypersonic Aerousurfaces: Theoretical Considerations and Historical Experience," *J. Mater. Sci.*, **39**, 5887–904 (2004).
- E. Wuchina, M. Opeka, S. Causey, K. Buesking, J. Spain, A. Cull, J. Routbort, and F. Gutierrez-Mora, "Designing for Ultrahigh-Temperature Applications: The Mechanical and Thermal Properties of HfB_2 , HfC_x , HfN_x , and $\alpha\text{-Hf(N)}$," *J. Mater. Sci.*, **39**, 5939–49 (2004).
- E. Opila, S. Levine, and J. Lorincz, "Oxidation of ZrB_2 and HfB_2 -Based Ultra-High Temperature Ceramics: Effect of Ta Additions," *J. Mater. Sci.*, **39** [19] 5969–77 (2004).
- W. G. Fahrenholtz, G. E. Hilmas, A. L. Chamberlain, and J. W. Zimmermann, "Processing and Characterization of ZrB_2 -Based Ultra-High Temperature Monolithic and Fibrous Monolithic Ceramics," *J. Mater. Sci.*, **39** [19] 5951–7 (2004).
- W. G. Fahrenholtz, "The ZrB_2 Volatility Diagram," *J. Amer. Ceram. Soc.*, **88** [12] 3509–12 (2005).
- L. Kaufman and E. Clougherty, "Investigation of Boride Compounds for Very High Temperature Applications — Part I," Technical Report RTD-TDR-63-4096: AFML, WPAFB, OH, December, 1963.
- L. Kaufman and E. Clougherty, "Investigation of Boride Compounds for Very High Temperature Applications — Part II," Technical Report RTD-TDR-63-4096 : Part 2, AFML, WPAFB, OH, February, 1965.
- E. V. Clougherty, R. L. Pober, and L. Kaufman, "Synthesis of Oxidation-Resistant Metal Diboride Composites," *Trans. Met. Soc. AIME*, **242**, 1077–82 (1968).
- J. R. Fenter, "Refractory Diborides as Engineering Materials," *SAMPE Quarterly*, **2** [3] 1–15 (1971).
- J. B. Berkowitz-Mattuck, "High-Temperature Oxidation III : Zirconium and Hafnium Diborides," *J. Electrochem. Soc.*, **113**, 908–14 (1966).
- W. C. Tripp and H. C. Graham, "Thermogravimetric Study of the Oxidation of ZrB_2 in the Temperature Range of 800° to 1500°C ," *J. Electrochem. Soc.*, **118** [7] 1195–9 (1971).
- T. A. Parthasarathy, R. A. Rapp, M. Opeka, and R. J. Kerans, "A Model for the Oxidation of ZrB_2 , HfB_2 and TiB_2 ," *Acta Mater.*, **55**, 5999–6010 (2007).
- T. A. Parthasarathy, R. A. Rapp, M. Opeka, and R. J. Kerans, "A Model for Transitions in Oxidation Regimes of ZrB_2 ," *Mater. Sci. Forum*, **595–598**, 823–32 (2008).
- H. C. Graham and H. H. Davis, "Oxidation/Vaporization Kinetics of Cr_2O_3 ," *J. Am. Ceram. Soc.*, **54** [2] 89–93 (1971).

¹⁵A. W. Smith, F. W. Meszaros, and C. D. Amata, "Permeability of Zirconia, Hafnia and Thoria to Oxygen," *J. Am. Ceram. Soc.*, **49** [5] 240–4 (1966).

¹⁶C. Wagner, "Equations for Transport in Solid Oxides and Sulfides of Transition Metals," *Prog. Solid State Chem.*, **10** [1] 3–16 (1975).

¹⁷R. H. Perry and C. H. Chilton, *Chemical Engineers' Handbook*. McGraw-Hill Book Company, New York, NY, 1973.

¹⁸I. Barin, *Thermochemical Data of Pure Substances I*, 3rd edition, VCH Verlagsgesellschaft, New York, 1995.

¹⁹R. A. Svehla, "Estimated viscosities and thermal conductivities of gases at high temperatures," NASA Technical report R-132, 1962.

²⁰R. A. Eppler, "Viscosity of Molten B₂O₃," *J. Am. Ceram. Soc.*, **49** [12] 679–80 (1966).

²¹P.-C. Li, A. C. Ghose, and G.-J. Su, "Viscosity Determination of Boron Oxide and Binary Borates," *J. Am. Ceram. Soc.*, **45** [2] 83–8 (1962).

²²T. Tokuda, T. Ido, and T. Yamaguchi, "Self Diffusion in a Glassformer Melt. Oxygen Transport in Boron Trioxide," *Z. Naturforschung.*, **26A**, 2058–60 (1971).

²³K. L. Luthra, "Oxidation of Carbon/Carbon composites—A Theoretical Analysis," *Carbon*, **26**, 217–24 (1988).

²⁴N. Wakao and J. M. Smith, "Diffusion in Catalyst Pellets," *Chem. Eng. Sci.*, **17** [11] 825–34 (1962).

²⁵C. N. Scatterfield, *Mass Transfer in Heterogenous Catalysis*. MIT Press, Cambridge, MA, 1970.

²⁶J. M. Zalc, S. C. Reyes, and E. Iglesia, "The Effects of Diffusion Mechanism and Void Structure on Transport Rates and Tortuosity Factors in Complex Porous Structures," *Chem. eng. Sci.*, **59**, 2947–60 (2004).

²⁷C. Wang, M. Zinkevich, and F. Aldinger, "The ZrO₂–HfO₂ System: DTA Measurements and Thermodynamic Calculations," *J. Am. Ceram. Soc.*, **89** [12] 3751–8 (2006).

²⁸D. Taylor, "Thermal Expansion Data: II Binary Oxides with Fluorite and Rutile Structures, Mo₂, and the Antifluorite Structure, M₂O," *Br. Ceram. Trans.*, **83** [2] 32–7 (1984).

²⁹W. D. Kingery, "Surface Tension of Some Liquid Oxides and their Temperature Coefficients," *J. Am. Ceram. Soc.*, **42** [1] 6–10 (1959).

³⁰L. Kaufman, E. V. Clougherty, and J. B. Berkowitz-Mattuck, "Oxidation Characteristics of Hafnium and Zirconium Diboride," *Trans. of Met. Soc. AIME*, **239**, 458–66 (1967). □